Nawras Haidar*, Salwan Obaid* Mohamed Jawad*

سرعة دخول حرجة للمائع المتدفق. تم الحصول على زيادة طفيفة نسبياً في تردد الهيكل عند زيادة ضغط المائع الداخل. بالاضافة الى ذلك كان هناك سمك مثالي للانبوب و لكل سرعة تدفق للمائع و التي تؤدي الى الحصول على اقصى خواص ديناميكية.

كلمات رئيسية: خط انابيب ذات زاويه، عنصر محدد، جريان مائع، السرعة الحرجة، التردد الطبيعي.

1. INTRODUCTION

The dynamics and stability of pipes conveying fluid have been studied extensively over the past 60 years, because of its growing importance in aerospace and nuclear fields such as vibrations of heat exchangers, liquid-fuel rocket piping, and nuclear reactor coolant channels. Generally, fluid flow through a pipe can impose a pressure on the internal wall of the pipe causing to deflect it under certain flow conditions. Due to this flow, an internal reaction force is produced that leading to curve the pipe and conform the fluid at any instant of motion. Due to acceleration of fluid and pipe masses, a gyroscopic effect is also presented. The gyroscopic effect always opposes the accelerated motion of the structure. The Coriolis force should be taken into consideration which resulted from relative motion between the pipe and fluid through its motion. These accompanying factors lead to increase the pipeline instability in different amounts.

Housner (1952) studied the flow induced vibration of a straight pipe by using Hamilton's principle. For a simply supported straight pipe, he found that the pipe may buckle, like a column subjected to axial loading, at a critical flow velocity. Benjamin (1961) and Gregory and Païdoussis (1966) modeled cantilevered pipe as a branch pipe and an elastic continuum pipe, respectively, to investigate the dynamic behaviors. Unny *et al.* (1970) studied the effect of curvature on the dynamic behaviors of curved pipes, and Chen (1972, 1973) analyzed curved pipes by investigating in-plane and out-of-plane vibrations. The effects of flow velocity and Coriolis force on the natural frequency were discussed. Mote (1971) studied the vibration and stability of cantilever pipe by finite element method using Ritz method, Hill and Davis (1974) investigated the vibration of the pipe with constant curvature by finite element method using Galerkin's method. Kohli and Nakva (1984) analyzed the straight and curved tubes conveying fluid by means of straight beam finite elements. Koo and Park (1996) investigated the vibration analysis of piping system conveying fluid by employing the wave approach. The straight pipe elements conveying fluid were formulated using a dynamic stiffness matrix in the frequency domain. The curved pipe sections were treated with a single curved pipe element utilizing the mixed methodology of the dynamic stiffness method and the transfer matrix method. Lee *et al.* (1996) presented a transfer matrix formulation for three dimensional vibration analysis of straight and curved piping systems containing fluid flow with small computer core memory usage. Nadeem (2001) studied the dynamics behavior of pipelines using finite element method taking into consideration the dynamics effects of Coriolis force on a fluid filled pipeline. His study was limited to in plane vibration of pipeline. Lee and Chung (2002) investigated a new non-linear model of a straight pipe conveying fluid where the pipe is fixed at both ends. Jung (2008) analyzed the in-plane and out-of-plane motions of a semi-circular pipe conveying fluid. Assuming that the centerline of the semi-circular pipe was extensible, nonlinear equations of in-plane and out-of-plane motions are derived according to the extended Hamilton's principle. The derived equations of motion were discretized by applying the Galerkin method. Linearized

equations around the equilibrium position were obtained from the discretized equations, and then the dynamic characteristics of the pipe were investigated. Rinaldi (2009) investigated the dynamics and stability of cantilevered structures subjected to internal, external, or simultaneous internal and external axial flows. This was accomplished, in some cases, by deriving the linear equations of motion using a Newtonian approach and, in other cases, by making the necessary modifications to existing theoretical models. The continuous cantilevered systems were then discretized using the Galerkin method in order to determine their complex eigen frequencies. Moreover, numerous experiments were performed to compare and validate, or otherwise, the theoretical models proposed. Huang *et al*. (2010) applied the eliminated element-Galerkin method to calculate the natural frequency with different boundary conditions on the basis of typical transverse vibration model. Then, the relationship between simplified natural frequency of the pipeline and that of Euler beam was discussed. In a given boundary condition, the four components (mass, stiffness, length and flow velocity) which relate to the natural frequency of pipeline conveying fluid were studied in detail and the results indicate that the effect of Coriolis force on natural frequency was inappreciable. Meng *et al*. (2011) investigated the three-dimensional nonlinear dynamics of a fluid-conveying pipe undergoing overall motions. The nonlinear differential equations were solved using Ritz method. Ni *et al*. (2011) analyzed the free vibration problem of pipes conveying fluid with several typical boundary conditions using differential transformation method. It is demonstrated that the differential transformation method has high precision and computational efficiency in the vibration analysis of pipes conveying fluid.

In this paper, an angled pipeline composed of two straight pipes connected by an elbow are constructed in three-dimensional space and analyzed by finite element method. A fixed-fixed pipeline end conditions will be adopted in this study. The mass, stiffness, damping (Coriolis) matrices are derived and the eigenvalue analysis is then performed. The forces occur due to momentum change and pressure when the fluid pass by the elbow part is considered.

2. EQUATION OF MOTION

The differential equation of motion for three dimensions vibration of a frame pipe carrying a moving fluid is given by (Païdoussis, 2004)

$$EI_y \frac{\partial^4 w}{\partial x^4} + EI_z \frac{\partial^4 v}{\partial x^4} + \{MU^2 + (pA_i - Fx)\}[\frac{\partial^2 w}{\partial x^2} + \frac{\partial^2 v}{\partial x^2}] + 2MU[\frac{\partial^2 w}{\partial x \partial t} + \frac{\partial^2 v}{\partial x \partial t}] + (m+M)[\frac{\partial^2 w}{\partial t^2} + \frac{\partial^2 v}{\partial t^2}] + EA_p \frac{\partial^2 u}{\partial x^2} + GJ \frac{\partial^2 \theta}{\partial x^2} + (m+M)[\frac{\partial^2 u}{\partial t^2} + r^2 \frac{\partial^2 \theta}{\partial t^2}] = 0 \quad (1)$$

Where u, w, and v are the coordinate axes in the directions of x, y, and z respectively, θ is the pipe angular displacement, E and G are the pipe axial and shear moduli of elasticity respectively, I_y and I_z are moment of inertia of the pipe in y and z directions respectively, J is the pipe polar moment of inertia, m = mass of the pipe per unit length, conveying fluid of mass per unit length (M), U is the steady mean flow velocity of fluid with respect to pipe, x = coordinate measured along the pipe length, Fx is the tension force in the pipe, A_p, A_i, r are the cross section pipe area, internal pipe area (fluid area), and pipe radius of gyration respectively. **Fig.(1)** shows a simple

Nawras Haidar*, Salwan Obaid* Mohamed Jawad*

representation, in three dimensional space, of the problem within hand which is consist of two pipe joint at their junction by an elbow.

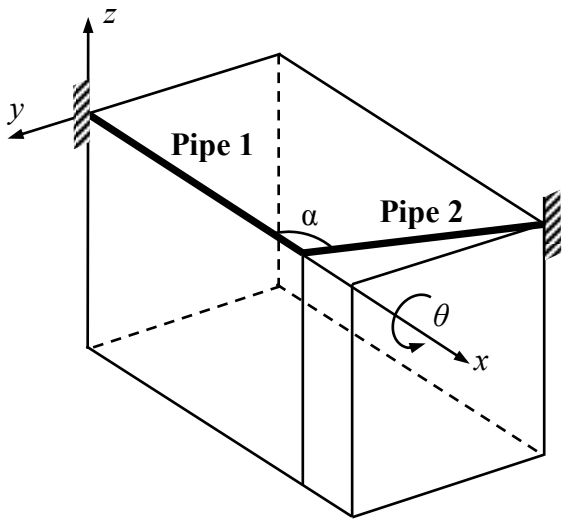

Fig.(1): Pipeline Model.

3. FINITE ELEMENTS DISCRETIZATION

In **Fig.(2)**, i and j represent the node points of finite element of length (l). Each node point has 6 degrees of freedom which consist of 3 linear displacements u, w, v and 3 rotational displacements θ_x , θ_y ,θ_z. Therefore the finite element has the total 12 degrees of freedom.

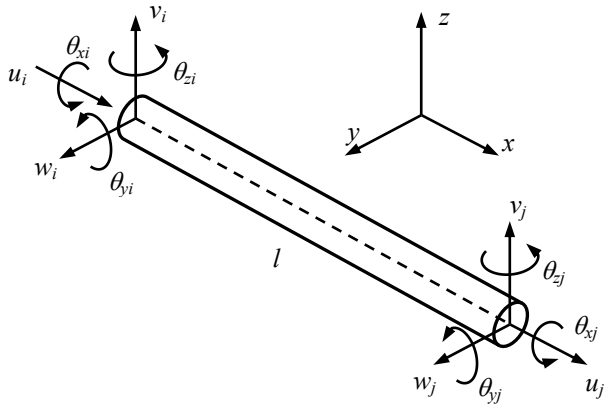

Fig.(2): Degree of freedom of pipe element.

The element displacement vector for a pipe element in space can be written as

$$\{q\}^T = \{u_1 \quad w_1 \quad v_1 \quad \theta_{x1} \quad \theta_{y1} \quad \theta_{z1} \quad u_2 \quad w_2 \quad v_2 \quad \theta_{x2} \quad \theta_{y2} \quad \theta_{z2}\} \tag{2}$$

For transverse (flexural) pipe vibration, the shape functions are (Rao, 2004)

$$\left.\begin{aligned} N_1 &= \frac{1}{l^3}(2x^3 - 3lx^2 + l^3) \\ N_2 &= \frac{1}{l^2}(x^3 - 2lx^2 + l^2 x) \\ N_3 &= \frac{1}{l^3}(3lx^2 - 2x^3) \\ N_4 &= \frac{1}{l^2}(x^3 - lx^2) \end{aligned}\right\} \quad (3)$$

While, for axial and torsional vibrations the shape functions are

$$\left.\begin{aligned} N_5 &= (1 - \frac{x}{l}) \\ N_6 &= (\frac{x}{l}) \end{aligned}\right\} \quad (4)$$

The displacement models can be expressed as

- For transverse displacements

$$w(x) = v(x) = \sum_{k=1}^{4} N_k(x) q_k \quad (5)$$

- For axial and torsional displacements

$$u(x) = \theta_x(x) = \sum_{k=5}^{6} N_k(x) q_k \quad (6)$$

The kinetic energy of pipe element is equal to

$$KE = \underbrace{\tfrac{1}{2}\int_0^l (m+M)(\frac{\partial w}{\partial t})^2 dx}_{transverse,\ \ y-dir.} + \underbrace{\tfrac{1}{2}\int_0^l (m+M)(\frac{\partial v}{\partial t})^2 dx}_{transverse,\ \ z-dir.} + \underbrace{\tfrac{1}{2}\int_0^l (m+M)(\frac{\partial u}{\partial t})^2 dx}_{axial} + \underbrace{\tfrac{1}{2}\int_0^l (m+M) r^2 (\frac{\partial \theta_x}{\partial t})^2 dx}_{torsional} \quad (7)$$

After finding the individual mass matrices for each term in the above equation, the total arranged mass matrix, according to displacement vector [eq. (2)], of pipe element in space has the following form

$$\hat{m} = \frac{(m+M)l}{420} \begin{bmatrix} 140 & 0 & 0 & 0 & 0 & 0 & 70 & 0 & 0 & 0 & 0 & 0 \\ 0 & 156 & 0 & 0 & 0 & 22l & 0 & 54 & 0 & 0 & 0 & -13l \\ 0 & 0 & 156 & 0 & -22l^2 & 0 & 0 & 0 & 54 & 0 & 13l & 0 \\ 0 & 0 & 0 & 140r^2 & 0 & 0 & 0 & 0 & 0 & 70r^2 & 0 & 0 \\ 0 & 0 & -22l^2 & 0 & 4l^2 & 0 & 0 & 0 & -13l & 0 & -3l^2 & 0 \\ 0 & 22l & 0 & 0 & 0 & 4l^2 & 0 & 13l & 0 & 0 & 0 & -3l^2 \\ 70 & 0 & 0 & 0 & 0 & 0 & 140 & 0 & 0 & 0 & 0 & 0 \\ 0 & 54 & 0 & 0 & 0 & 13l & 0 & 156 & 0 & 0 & 0 & -22l \\ 0 & 0 & 54 & 0 & -13l & 0 & 0 & 0 & 156 & 0 & 22l & 0 \\ 0 & 0 & 0 & 70r^2 & 0 & 0 & 0 & 0 & 0 & 140r^2 & 0 & 0 \\ 0 & 0 & 13l & 0 & -3l^2 & 0 & 0 & 0 & 22l & 0 & 4l^2 & 0 \\ 0 & -13l & 0 & 0 & 0 & -3l^2 & 0 & -22l & 0 & 0 & 0 & 4l^2 \end{bmatrix} \quad (8)$$

While the potential energy is

$$PE=\underbrace{\tfrac{1}{2}\int_0^l EI_y(\frac{\partial^2 w}{\partial x^2})^2dx}_{transverse,\ \ y-dir.}+\underbrace{\tfrac{1}{2}\int_0^l EI_z(\frac{\partial^2 v}{\partial x^2})^2dx}_{transverse,\ \ z-dir.}+\underbrace{\tfrac{1}{2}\int_0^l EA_p(\frac{\partial u}{\partial x})^2dx}_{axial}+\underbrace{\tfrac{1}{2}\int_0^l GJ(\frac{\partial \theta_x}{\partial x})^2dx}_{torsional} \tag{9}$$

This will lead to the following symmetry pipe stiffness matrix

$$k_1=\begin{bmatrix}
\frac{EA_p}{l} & 0 & 0 & 0 & 0 & 0 & -\frac{EA_p}{l} & 0 & 0 & 0 & 0 & 0\\
0 & \frac{12EI_z}{l^3} & 0 & 0 & 0 & \frac{6EI_z}{l^2} & 0 & -\frac{12EI_z}{l^3} & 0 & 0 & 0 & \frac{6EI_z}{l^2}\\
0 & 0 & \frac{12EI_y}{l^3} & 0 & -\frac{6EI_y}{l^2} & 0 & 0 & 0 & -\frac{12EI_y}{l^3} & 0 & -\frac{6EI_y}{l^2} & 0\\
0 & 0 & 0 & \frac{GJ}{l} & 0 & 0 & 0 & 0 & 0 & -\frac{GJ}{l} & 0 & 0\\
0 & 0 & -\frac{6EI_y}{l^2} & 0 & \frac{4EI_y}{l} & 0 & 0 & 0 & \frac{6EI_y}{l^2} & 0 & \frac{2EI_y}{l} & 0\\
0 & \frac{6EI_z}{l^2} & 0 & 0 & 0 & \frac{4EI_z}{l} & 0 & -\frac{6EI_z}{l^2} & 0 & 0 & 0 & \frac{2EI_z}{l}\\
-\frac{EA_p}{l} & 0 & 0 & 0 & 0 & 0 & \frac{EA_p}{l} & 0 & 0 & 0 & 0 & 0\\
0 & -\frac{12EI_z}{l^3} & 0 & 0 & 0 & -\frac{6EI_z}{l^2} & 0 & \frac{12EI_z}{l^3} & 0 & 0 & 0 & -\frac{6EI_z}{l^2}\\
0 & 0 & -\frac{12EI_y}{l^3} & 0 & \frac{6EI_y}{l^2} & 0 & 0 & 0 & \frac{12EI_y}{l^3} & 0 & \frac{6EI_y}{l^2} & 0\\
0 & 0 & 0 & -\frac{GJ}{l} & 0 & 0 & 0 & 0 & 0 & \frac{GJ}{l} & 0 & 0\\
0 & 0 & -\frac{6EI_y}{l^2} & 0 & \frac{2EI_y}{l} & 0 & 0 & 0 & \frac{6EI_y}{l^2} & 0 & \frac{4EI_y}{l} & 0\\
0 & \frac{6EI_z}{l^2} & 0 & 0 & 0 & \frac{2EI_z}{l} & 0 & -\frac{6EI_z}{l^2} & 0 & 0 & 0 & \frac{4EI_z}{l}
\end{bmatrix} \tag{10}$$

The term ($\{MU^2+(pA_i-Fx)\}[(\frac{\partial^2 w}{\partial x^2})+(\frac{\partial^2 v}{\partial x^2})]$) in eq.(1) has a potential energy that can be represented as:

$$PE=\tfrac{1}{2}\int_0^l\{MU^2+(pA_i-Fx)\}(\frac{\partial w}{\partial x})(\frac{\partial w}{\partial x})dx+\tfrac{1}{2}\int_0^l\{MU^2+(pA_i-Fx)\}(\frac{\partial v}{\partial x})(\frac{\partial v}{\partial x})dx \tag{11}$$

Leading to symmetry matrix (k_2), which contains the force per unit length (stiffness unit) that conforms the fluid to the pipe (weakening effect) besides the axial tension force (stiffening effect).

$$k_2=\frac{MU^2+pA_i-Fx}{30l}\begin{bmatrix}
0 & 0 & 0 & 0 & 0 & 0 & 0 & 0 & 0 & 0 & 0 & 0\\
0 & 36 & 0 & 0 & 0 & 3l & 0 & -36 & 0 & 0 & 0 & 3l\\
0 & 0 & 36 & 0 & 3l & 0 & 0 & 0 & -36 & 0 & 3l & 0\\
0 & 0 & 0 & 0 & 0 & 0 & 0 & 0 & 0 & 0 & 0 & 0\\
0 & 0 & 3l & 0 & 4l^2 & 0 & 0 & 0 & -3l & 0 & -l^2 & 0\\
0 & 3l & 0 & 0 & 0 & 4l^2 & 0 & -3l & 0 & 0 & 0 & -l^2\\
0 & 0 & 0 & 0 & 0 & 0 & 0 & 0 & 0 & 0 & 0 & 0\\
0 & -36 & 0 & 0 & 0 & -3l & 0 & 36 & 0 & 0 & 0 & -3l\\
0 & 0 & -36 & 0 & -3l & 0 & 0 & 0 & 36 & 0 & -3l & 0\\
0 & 0 & 0 & 0 & 0 & 0 & 0 & 0 & 0 & 0 & 0 & 0\\
0 & 0 & 3l & 0 & -l^2 & 0 & 0 & 0 & -3l & 0 & 4l^2 & 0\\
0 & 3l & 0 & 0 & 0 & -l^2 & 0 & -3l & 0 & 0 & 0 & 4l^2
\end{bmatrix} \tag{12}$$

Here, we will call the above matrix as a *contradictory* matrix because it contains two opposite component effects. Where *Fx* is an axial tension force that caused by the change in fluid's momentum and pressure in a pipe bend (elbow). **Fig.(3)** shows the induced axial tension forces in the pipe bend.

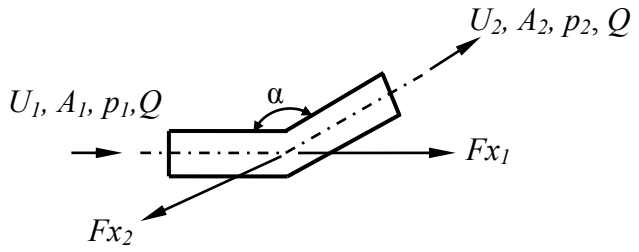

Fig.(3): Tension forces in pipe bend.

From **Fig.(3)**, the axial tension forces in pipe bend are equal to (Munson *et al*., 2002):

$$Fx_1 = p_1 A_1 + p_2 A_2 \cos(\alpha) + \rho_{fluid} Q[U_1 + U_2 \cos(\alpha)] \tag{13}$$

and

$$Fx_2 = R\{\frac{\sin(\psi)}{\sin(\alpha)}\} \tag{14}$$

where

$$R = [Fx_1^{\,2} + Fy^2]^{\frac{1}{2}}$$

$$Fy = p_2 A_2 \sin(\alpha) + \rho_{fluid} U_2 Q \sin(\alpha)$$

$$Q = U_1 A_1 = U_2 A_2$$

$$p_2 = p_1 + \rho_{fluid}\{\frac{(U_1^2 - U_2^2)}{2}\}$$

$$\psi = \tan^{-1}\{\frac{\sin(\alpha)}{1+\cos(\alpha)}\}$$

From the mathematical formulation presented above, it is clear that the overall stiffness is composed of two parts, namely the contradictory and pipe structural stiffness matrices.

The term ($2MU[\frac{\partial^2 w}{\partial x \partial t} + \frac{\partial^2 v}{\partial x \partial t}]$) in eq.(1) is the inertial force associated with the Coriolis acceleration arising from the fluid flows with velocity *U* relative to the pipe. This term has a dissipation energy which is equal to

$$DE = \tfrac{1}{2}\int_0^l 2MU(\frac{\partial w}{\partial x})(\frac{\partial w}{\partial t})dx + \tfrac{1}{2}\int_0^l 2MU(\frac{\partial v}{\partial x})(\frac{\partial v}{\partial t})dx \tag{15}$$

This gives a skew-symmetry damping matrix

$$C=\frac{MU}{30}\begin{bmatrix} 0 & 0 & 0 & 0 & 0 & 0 & 0 & 0 & 0 & 0 & 0 & 0 \\ 0 & -30 & 0 & 0 & 0 & -6l & 0 & -30 & 0 & 0 & 0 & 6l \\ 0 & 0 & -30 & 0 & -6l & 0 & 0 & 0 & -30 & 0 & 6l & 0 \\ 0 & 0 & 0 & 0 & 0 & 0 & 0 & 0 & 0 & 0 & 0 & 0 \\ 0 & 0 & 6l & 0 & 0 & 0 & 0 & 0 & -6l & 0 & l^2 & 0 \\ 0 & 6l & 0 & 0 & 0 & 0 & 0 & -6l & 0 & 0 & 0 & l^2 \\ 0 & 0 & 0 & 0 & 0 & 0 & 0 & 0 & 0 & 0 & 0 & 0 \\ 0 & 30 & 0 & 0 & 0 & 6l & 0 & 30 & 0 & 0 & 0 & -6l \\ 0 & 0 & 30 & 0 & 6l & 0 & 0 & 0 & 30 & 0 & -6l & 0 \\ 0 & 0 & 0 & 0 & 0 & 0 & 0 & 0 & 0 & 0 & 0 & 0 \\ 0 & 0 & -6l & 0 & -l^2 & 0 & 0 & 0 & 6l & 0 & 0 & 0 \\ 0 & -6l & 0 & 0 & 0 & -l^2 & 0 & 6l & 0 & 0 & 0 & 0 \end{bmatrix} \tag{16}$$

It can be seen that the 12 * 12 element matrices given in eqs. (8), (10), (12) and (16) are with respect to the local *xyz* coordinate system. Since the nodal displacements for the angled pipe are in different local coordinates, thus it must transform the local coordinate to global coordinate system. The transformation matrix, λ, can be identified as (Rao, 2004);

$$\lambda=\begin{bmatrix} l_{ox} & m_{ox} & n_{ox} & 0 & 0 & 0 & 0 & 0 & 0 & 0 & 0 & 0 \\ l_{oy} & m_{oy} & n_{oy} & 0 & 0 & 0 & 0 & 0 & 0 & 0 & 0 & 0 \\ l_{oz} & m_{oz} & n_{oz} & 0 & 0 & 0 & 0 & 0 & 0 & 0 & 0 & 0 \\ 0 & 0 & 0 & l_{ox} & m_{ox} & n_{ox} & 0 & 0 & 0 & 0 & 0 & 0 \\ 0 & 0 & 0 & l_{oy} & m_{oy} & n_{oy} & 0 & 0 & 0 & 0 & 0 & 0 \\ 0 & 0 & 0 & l_{oz} & m_{oz} & n_{oz} & 0 & 0 & 0 & 0 & 0 & 0 \\ 0 & 0 & 0 & 0 & 0 & 0 & l_{ox} & m_{ox} & n_{ox} & 0 & 0 & 0 \\ 0 & 0 & 0 & 0 & 0 & 0 & l_{oy} & m_{oy} & n_{oy} & 0 & 0 & 0 \\ 0 & 0 & 0 & 0 & 0 & 0 & l_{oz} & m_{oz} & n_{oz} & 0 & 0 & 0 \\ 0 & 0 & 0 & 0 & 0 & 0 & 0 & 0 & 0 & l_{ox} & m_{ox} & n_{ox} \\ 0 & 0 & 0 & 0 & 0 & 0 & 0 & 0 & 0 & l_{oy} & m_{oy} & n_{oy} \\ 0 & 0 & 0 & 0 & 0 & 0 & 0 & 0 & 0 & l_{oz} & m_{oz} & n_{oz} \end{bmatrix} \tag{17}$$

Here, l_{ox}, m_{ox}, and n_{ox} denote the direction cosines of the *x*-axis; l_{oy}, m_{oy} , and n_{oy} represent the direction cosines of the *y*-axis; and l_{oz}, m_{oz}, and n_{oz} indicate the direction cosines of the *z*-axis with respect to the global axes. This leads to the following global element matrices:

$$[\hat{m}]_{Global}=[\lambda]^T[\hat{m}][\lambda] \tag{18}$$

$$[k_{overall}]_{Global}=[\lambda]^T[k_{overall}][\lambda] \tag{19}$$

$$[C]_{Global}=[\lambda]^T[C][\lambda] \tag{20}$$

4. DYNAMIC ANALYSIS

The standard equation of motion in the finite element form is

$$[\hat{m}]_{Global}\{\ddot{q}\}+[C]_{Global}\{\dot{q}\}+[k_{overall}]_{Global}\{q\}=\{0\} \quad (21)$$

Where $k_{overall}=(k_{1,overall}-k_{2,overall})$

Since the above equation has a damping term with skew-symmetric characteristic, thus the solution of eigenvalues problem should be executed to the characteristic matrix $[\Omega]$ (Meirovitch, 1980), which is equal to

$$[\Omega]=\begin{bmatrix}[0] & [I]\\ -[\hat{m}]^{-1}[k_{overall}] & -[\hat{m}]^{-1}[C]\end{bmatrix}_{Global} \quad (22)$$

The solution of eigenvalue problem yields complex roots. The imaginary part of these roots represents the natural frequencies of damped system. The real part indicates the rate of decay of the free vibration.

5. RESULTS AND DISCUSSION

Fig.(4) shows the effect of frame angle on the critical velocity of fluid. It is clear that any increase in frame angle will lead to decrease the critical flow velocity, i.e. accelerate the instability of structure. This behavior is mainly caused by decreasing the axial tension forces in the pipe bend, which play a stiffening role, with increasing the frame angle. The important note is that when the frame angle converges to 90^{o}. At this angle, the critical flow velocity goes to reach an infinite value where the contradictory matrix (k_2) is vanished. This behavior was confirmed previously by the works that done by (Koo *et al*., 1996 and Lee *et al*., 1996).

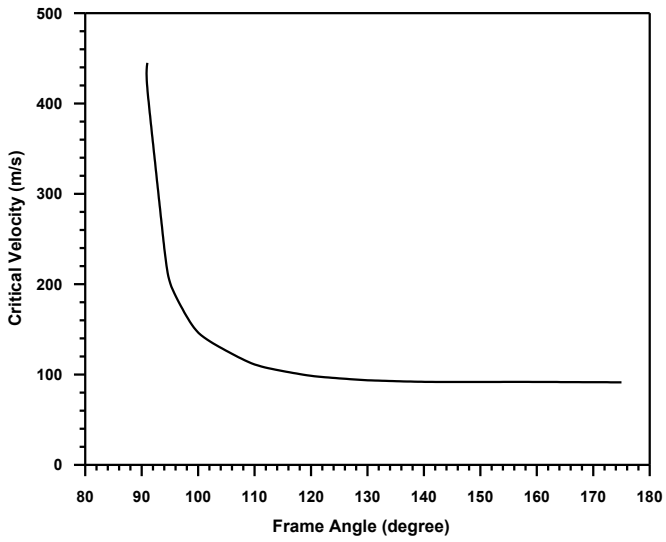

Fig.(4): Effect of frame angle on critical velocity of fluid.

Pipe lengths L_1 and L_2 are (2 m), fluid density is (1000 kg/m^3), pipe density is (8000 kg/m^3), thicknesses of pipes are (0.001 m), outer diameters of the pipes are (0.03 m), elastic modulus of pipe is (207 GPa).

Fig.(5) presents the effect of pipe lengths ratio on the critical flow velocity with different frame angles. Any increase in this ratio leads to decrease the critical velocity of flowing. The main reason of this behavior is that the fame structure becomes heavier in weight and weaker in its stiffness with increasing frame length ratio. Moreover, the curves behave to converge when the value of this ratio reaching one and will continue in compactness after this value.

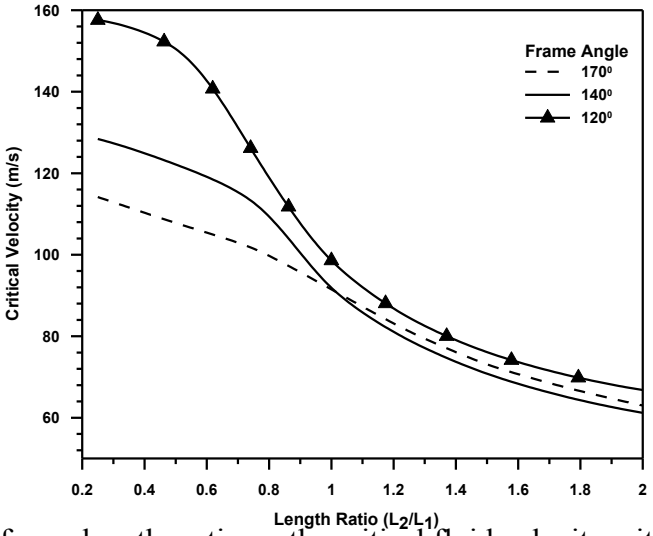

Fig.(5): Effect of frame lengths ratio on the critical fluid velocity with different frame angles. *Pipe length L_1 is (2 m), fluid density is (1000 kg/m^3), pipe density is (8000 kg/m^3), thicknesses of pipes are (0.001 m), outer diameters of the pipes are (0.03 m), elastic modulus of pipe is (207 GPa).*

Figs.(6-a, b and **c)** show the effect of inlet fluid velocity on the fundamental frame frequency with different diameters ratios and different frame angles. In general, increasing the inlet fluid velocity leads in turn to weaken the frame frequency. The unexpected behavior is executed by the frame with angle equal or larger than 170^o for all pipe diameter ratios accept unity. Where in **Fig.(6-a)** and at relatively low inlet fluid velocity about (11 m/s), the frame frequency tends to reduce with increasing the inlet fluid velocity and then after this behavior is reversed. Further increasing in inlet fluid velocity leads to dramatic drop in frequency. This behavior can be depicted as an alternative one. Where, at relatively low inlet velocity, the force conforms fluid (weakening effect) seems to be larger than the axial tension forces (stiffening effect) generated in the pipe frame. With further increase in flow velocity, the values of these effects will be reversed i.e. stiffening effect becomes larger than weakening effect. The values of axial tension forces components are very sensitive to frame angle and pipes sections (pipe diameters ratio).

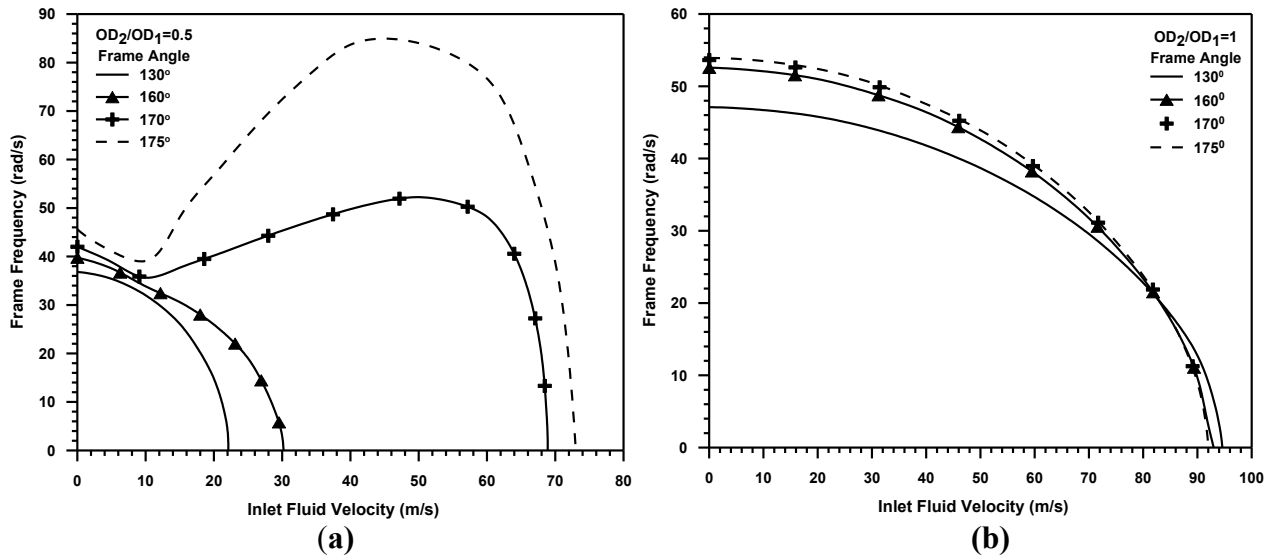

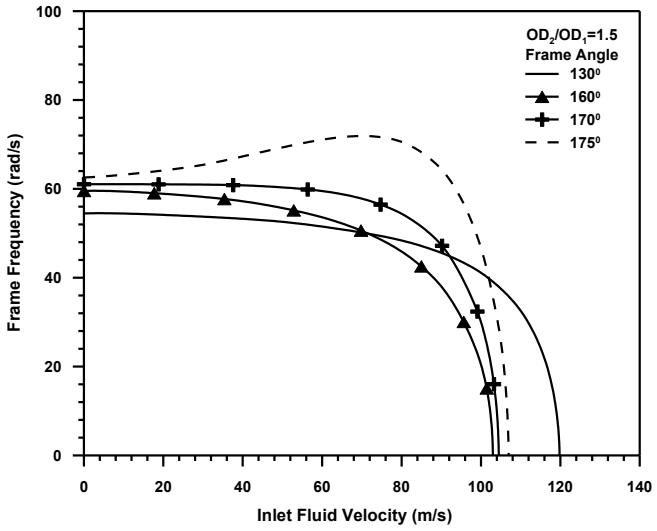

(c)

Fig.(6): Effect of inlet fluid velocity on the frame frequency with different diameters ratio and different frame angles.

Pipe lengths L_1 and L_2 are (2 m), fluid density is (1000 kg/m^3), pipe density is (8000 kg/m^3), thicknesses of pipes are (0.001 m), outer diameter of the inlet pipe is (0.03 m), elastic modulus of pipe is (207 GPa), Inlet fluid pressure is (100 kPa).

In Fig.(7), the relation between diameters ratio and critical inlet velocity at different frame angles is shown. In this figure, the critical inlet velocities will rise continuously with increasing the diameters ratio and reaching maximum values, then after it will drops smoothly. It is well known that increasing the second pipe diameter leads to minimize the fluid velocity through this pipe (positive effect on the frame dynamic characteristics). At same time, the pipe will be heavier (negative effect on frame dynamic characteristics). The combination of these two effects gives a complex behavior. Also here, the frame with an angle of 170^o exhibits an alternative behavior for the reasons that clarified before.

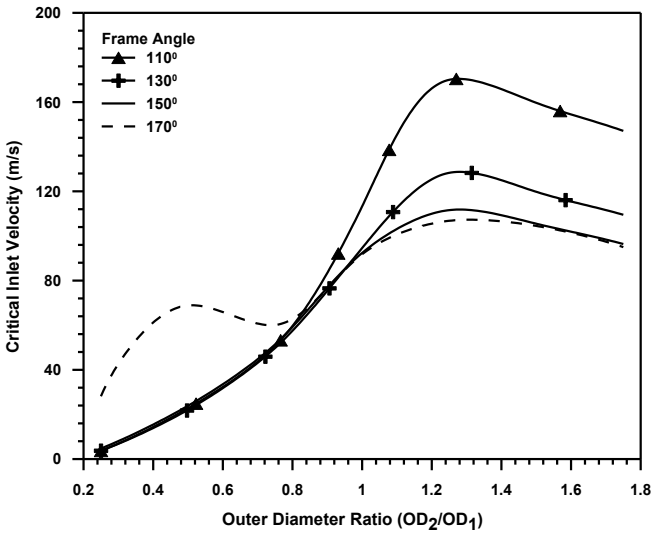

Fig.(7): Effect of outer diameters ratio on the critical fluid velocity at different frame angles.

Pipe lengths L_1 and L_2 are (2 m), fluid density is (1000 kg/m^3), pipe density is (8000 kg/m^3), thicknesses of pipes are (0.001 m), outer diameter of inlet pipe is (0.03 m), elastic modulus of pipe is (207 GPa), inlet fluid pressure is (100 kPa).

Fig.(8) shows the effect of inlet fluid velocity on the frame frequency with different inlet fluid pressures. Here, at same inlet velocity, the frame frequency will increase by little amount when increasing the inlet fluid pressure.

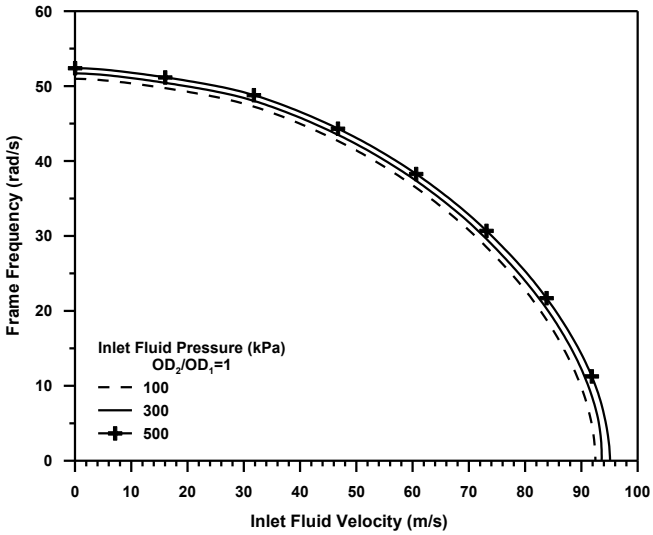

Fig.(8): Effect of inlet fluid velocity on the frame frequency with different inlet fluid pressures.

Pipe lengths L_1 and L_2 are (2 m), fluid density is (1000 kg/m^3), pipe density is (8000 kg/m^3), thicknesses of pipes are (0.001 m), frame angle (150^o), outer diameters of pipes are (0.03 m), elastic modulus of pipe is (207 GPa).

Fig.(9) presents the effect of pipe thickness on the frame frequency at different inlet fluid velocities. When the pipe thickness is relatively small, the effect of fluid velocity on the frame frequency is obvious. Increasing pipe thickness to certain values gives the best ever frame frequency for each fluid velocity. After that, the frame frequency will converge and drops smoothly. This behavior is mainly caused by increasing pipe stiffness and weight with thickness increasing. This means that there is an optimum pipe thickness for each flowing velocity that gives best ever frame frequency. The combined effects of these two parameters will control the dynamic behavior of the angled pipeline structures.

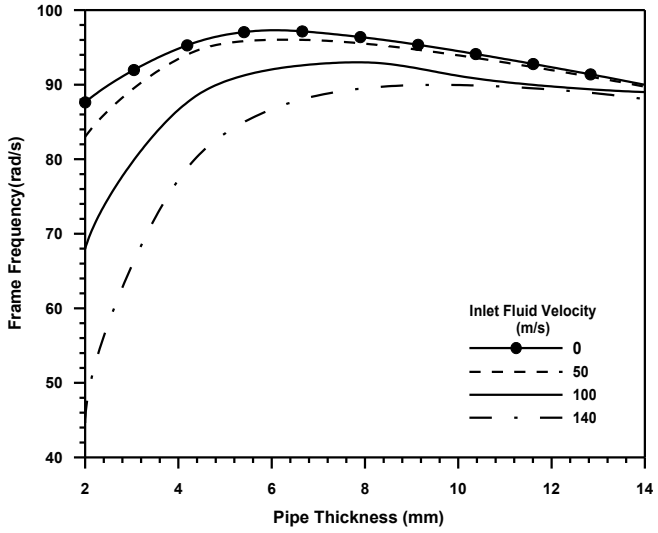

Fig.(9): Effect of pipe thickness on the frame frequency at different inlet fluid velocities.

Pipe lengths L_1 and L_2 are (2 m), fluid density is (1000 kg/m^3), pipe density is (8000 kg/m^3), frame angle (150^o), outer diameters of pipes are (0.05 m), elastic modulus of pipe is (207 GPa).

5. CONCLUSIONS

Through the theory and numerical simulations for the fluid conveying angled pipelines, the following conclusions are obtained:

1- Increasing frame angle from 90^o up to 180 ^{o} will lead to decrease the critical flow velocity of fluid.
2- The pipeline frame is always stable when it constructed with right angle.
3- In angled pipeline, a contradictory matrix is formed which consist of two opposite effects namely weakening and stiffening.
4- There is an optimum diameters ratio for each frame angle that gives the larger inlet critical velocity of fluid.
5- Increasing the frame inlet fluid pressure leads to relatively slight increase in its frequency.
6- For each fluid flow velocity, there is an optimum pipe thickness that gives the best dynamic characteristics.

REFERENCES

Benjamin, T. B., 1961, "Dynamics of System of Articulated Pipes Conveying Fluid, Parts I, II" Proc. of Royal Society (London), Ser. A 261, pp. 457-486.

Chen, S. S., 1972,"Vibration and Stability of a Uniformly Curved Tube Conveying Fluid", Journal of Acoustic Society of America , Vol. 51, No. 1 , Part 2, pp. 223-232.

Chen, S. S., 1973,"Out of-Plane Vibration and Stability of Curved Tubes Conveying Fluid", Journal of Applied Mechanics, Transaction of ASME, June, pp. 362-368.

Gregory, R. W. and Païdoussis, M. P., 1966, "Unstable Oscillation of Tubular Cantilevers Conveying Fluid; I., II", Proc. of Royal Society (London). Ser. A 293, pp. 512-527.

Hill, J. L., and Davis, C. G., 1974, "Effect of Initial Force on the Hydroelastic Vibration and Stability of Planar Curved Tubes," Journal of Applied Mechanics, Vo1.41, pp.355-359.

Housner, G. W, "Bending Vibrations of a Pipe Line Containing Flowing Fluid" journal of applied Mechanics, Vol.19, 1952, pp. 205-209.

Huang Y., Liu, Y., Li, B., Li, Y. and. Yue, Z , "Natural Frequency Analysis of Fluid Conveying Pipeline with Different Boundary Conditions" Nuclear Engineering and Design, Vol. 240, No.3, 2010, pp. 461- 467.

Jung, D., Chung, J., "In-Plane and Out-of-Plane Motions of an Extensible Semi-Circular Pipe Conveying Fluid" Journal of Sound and Vibration, Vol. 311, pp. 408-420, 2008.

Kohli, A .K., and Nakva, B. C., 1984, "Vibration Analysis of Straight and Curved Tubes Conveying Fluid by means of Straight Beam Finite Elements," Journal of Sound and Vibration, Vo1.93, pp.307-311.

Koo, G. H., and Park Y. S., "Vibration Analysis of a 3-Dimensional Piping System Conveying Fluid by Wave Approach" International journal of pressure vessels and piping, Vol.67, 1996, pp. 249-256.

Lee, D. M., Choi, M. J., and Oh. T. Y., "Transfer Matrix Modeling for the 3-Dimensional Vibration Analysis of Piping System Containing Fluid Flow" KSME Journal, Vol. 10, No. 2, pp. 180-189, 1996.

Lee S., and Chung J., "New Non-Linear Modeling for Vibration Analysis of a Straight Pipe Conveying Fluid ", Journal of Sound and Vibration, Vol. 254, 2002, 313-325.

Meirovitch, L., "Computational Methods in Structural Dynamics" Sijthoff and Noordhoff International Publisher, 1980.

Meng, D., Guo, H. Y., and Xu, S. P., "Non-Linear Dynamic Model of a Fluid-Conveying Pipe Undergoing Overall Motions" Applied Mathematical Modeling ,Vol.35,(2011), pp. 781–796.

Mote, C. D., 1971, "Non-conservative Stability by Finite Elements," Journal of the Engineering Mechanics Division, Proceeding of the American Society of Civil Engineers, pp. 645-656.

Munson, B. R., Young, D. F., and Okiishi, T. H., "Fundamentals of Fluid Mechanics" John Wiley and Sons, Fourth edition, 2002.

Nadeem, J., "Dynamics of Pipelines with a Finite Element Method" Msc. Thesis, University of Calgary, Alberta ,Canada, 2001.

Ni Q., Zhang, Z., and Wang, L., "Application of the Differential Transformation Method to Vibration Analysis of Pipes Conveying Fluid" Applied Mathematics and Computation, Vol. 217, 2011, pp. 7028- 7038.

Païdoussis, M. P., "Fluid-Structure Interactions", Vol. 2. Academic Press, London, 2004.

Rao, S. S.,"The Finite Element Method in Engineering" Fourth edition, Elsevier Science & Technology Books, 2004.

Rinaldi , S. "Experiments on the Dynamics of Cantilevered Pipes Subjected to Internal and/or External Axial Flow" Msc. Thesis, McGill University, Montreal ,Canada, 2009.

Unny. T. E., Martin, E. L., and Dubey, R. N., 1970, "Hydroelastic Instability of Uniformly Curved Pipe-Fluid Systems", Journal of Applied Mechanics, Transaction of ASME, Sep., pp. 817-822.

Nomenclatures

Symbol	Definition	Basic Unit
A_i	Fluid cross-sectional area	m^2
A_p	Pipe cross-sectional area	m^2
C	Damping matrix	-
E	Modulus of elasticity of pipe	N/m^2
Fx	Tension force in the pipe	N
G	Shear modulus of elasticity of pipe	N/m^2
I	Unity matrix	-
I_y, I_z	Pipe second moment of area in y and z directions	m^4
J	Polar second moment of area	m^4
k_1	Stiffness matrix of pipe	-
k_2	Contradictory matrix	-
L_1	Length of first pipe	m
L_2	Length of second pipe	m
l	Element length of pipe	m
M	Fluid mass per unit length	kg/m
m	Pipe mass per unit length	kg/m
$\hat{m}$	Pipe mass matrix	-
N_i	Shape function	-
OD	Outer diameter of pipe	m
p	Pressure inside the pipe	N/m^2
Q	Fluid discharge	m^3/s
r	Radius of gyration of pipe section	m
t	Time	s
U	Fluid velocity relative to the pipe	m/s

q	Displacement vector	-
$\dot{q}$	Velocity vector	-
$\ddot{q}$	Acceleration vector	-
x,y,z	Cartesian axes	-
α	Frame angle	degree
λ	Transformation matrix	-